Supporting Information

Biothiol-Triggered Hydrogen Sulfide (H_2S) Release from Near-Infrared Fluorescence H_2S Donor for Promoting Cutaneous Wound Healing

Xinyue Zhao[a,#], Mengbin Ding[c,#], Lulu Ning[d], Fang Yuan[a], Jingchao Li[c], Yuan Guo[a], Yuguang Mu[e], Jianjian Zhang[a,b,*]

[a] Key Laboratory of Synthetic and Natural Functional Molecule Chemistry of Ministry of Education, Key Lab of Modern Separation Science in Shaanxi Province, College of Chemistry and Materials Science, Northwest University, Xi'an, Shaanxi 710127, P. R. China

[b] Qinghai Provincial Key Laboratory of Salt Lake Resources Chemistry, Xining, 810008, P. R. China

[c] Shanghai Engineering Research Center of Nano-Biomaterials and Regenerative Medicine, College of Biological Science and Medical Engineering, Donghua University, Shanghai 201620, China

[d] Shaanxi Provincial Key Laboratory of Papermaking Technology and Specialty Paper Development, College of Bioresources Chemical and Materials Engineering, Shaanxi University of Science & Technology, Xi'an 710021, P. R. China

[e] School of Biological Sciences, Nanyang Technological University, 60 Nanyang Drive, Singapore 637551, Singapore

[#] These authors contributed equally to this work.

[*] Correspondence: orcid.org/0000-0002-5220-1280; Email: zhangjj@nwu.edu.cn (J. Zhang)

1. MATERIALS AND METHODS

1.1 Chemicals and Instruments

4-hydroxybenzaldehyde and tiophosgene were purchased from Aladdin (Shanghai, China). GSH, Cys, and Hcy were purchased from Sangon Biotech. Co., Ltd. (Shanghai, China). Lipopolysaccharide (LPS) was purchased from Sigma-Aldrich. Zebrafish were purchased from Shanghai FishBio. Co., Ltd. (Shanghai, China). Unless for special needs, all other reagents were obtained from qualified commercial suppliers and were used without further purification.

Fluorescence spectra were recorded on a fluorescence spectrophotometer (Shimadzu RF-5301, Japan). Absorption spectra were measured on a UV-visible spectrometer (Shimadzu UV-2550, Japan). Nuclear magnetic resonance (NMR) spectra were obtained using a Bruker Ascend 400 spectrometer operating at 400 MHz. The chemical shifts (δ) were referenced to residual DMSO (^{1}H NMR, 2.50 ppm), and $CHCl_3$ (^{1}H NMR, 7.26 ppm). High-resolution electrospray ionization mass spectra (HRMS) were measured on a Bruker micrOTOF-Q II mass spectrometer (Bruker Daltonics Corp., USA) with ESI mode. Fluorescence images of living cells were performed using a confocal laser scanning microscope (Nikon, A1). NO_2^- levels were obtained by using a Griess Reagent kit (Thermo Fisher Scientific) and absorbance at 550 nm was recorded by using a microplate reader ((BioTek, Synergy 2). The levels of pro-inflammatory cytokine (TNF-α and IL-6) were measured by an ELISA kit from Sangon Biotech (Shanghai, China), and absorbance at 450 nm was tested using a microplate reader (BioTek, Synergy 2). *In vivo* imaging in mice was performed using an IVIS Spectrum imaging system (Perkin Elmer, America).

1.2 Cell Culture and Cytotoxicity Test

RAW 246.7 cells were cultured at 37 °C under a humidified 5% CO_2 atmosphere in Dulbecco's modified Eagle's medium (DMEM), containing 10% heat-inactivated fetal bovine serum (FBS) and 1% penicillin/streptomycin. The cytotoxic effect of **PRO-ST** and TCOO was assessed by MTT assay. RAW 246.7 cells were incubated for 24 h upon different concentrations (0, 10.0, 20.0, 30.0, 40.0, and 50.0 μM) of **PRO-ST** and TCOO respectively. The cytotoxic effect (VR) of **PRO-ST**,

TCOO was assessed using the following equation: VR = $A/A_0 \times 100\%$, where A and A_0 are the absorbance of the experimental group and control group, respectively. The assays were performed in twelve sets for each concentration.

1.3 Confocal Microscopy Imaging in cells

RAW 246.7 cells were stained with DAPI (NucBlue Live Ready Probes Reagent, Thermo Fisher) for the nuclei as protocols. RAW 246.7 cells were firstly pretreated with NEM (1 mM) for 30 min at 37 °C, then the cells were treated with **PRO-ST** (10 μM) and exogenous thiols for another 30 min in DMEM, followed by washing with PBS twice before imaging. The cell imaging was carried out with the excitation/emission wavelength of 514/650±30 nm for **PRO-ST** and 405/450±20 nm for DAPI.

To investigate the H_2S release capacity of **PRO-ST**, fluorescent probe C-7AZ was used to image the release of H_2S in RAW 246.7 cells. The NEM-pretreated cells were incubated with **PRO-ST** (10 μM), Cys/Hcy/GSH (200 μM), and C-7AZ (3 μM) for 30 min. The cell imaging was carried out with the excitation/emission wavelength of 405/450±20 nm for C-7AZ.

1.4 Living Zebrafish imaging

The 3-day-old zebrafish were incubated in an E3 embryo medium for three days at 28 °C and were divided into five groups. In the experimental group, zebrafishes were cultured in an E3 embryo medium containing NEM (50 μM) for 30 min and then treated with **PRO-ST** (10 μM) and Cys (100 μM) for another 30 min. After washing three times with PBS buffer to remove the remaining medium, the zebrafish imaging was carried out with the excitation/emission wavelength of 514/650±40 nm for the red channel.

1.5 *In vivo* imaging of biothiols in mice

The 6-week-old mice (Kunming mice) were divided into three groups. The Control group was only given a subcutaneous injection of saline (25 μL); The second group was given a subcutaneous injection of **PRO-ST** (10 mM, 25 μL); The third group was first given a subcutaneous injection of NEM (100 mM, 25 μL) for 20 min and followed by subcutaneous injection of **PRO-ST** (10 mM, 25 μL) at the same

position. All groups were then imaged after 30 min with an excitation filter of 530 nm and an emission filter of 660 nm.

1.6 Anti-inflammatory protocols of PRO-ST and Control Compounds

Macrophage RAW 264.7 cells were seeded in a 24-well plate (5×10^5 cells/well) containing 0.5 mL of DMEM and incubated at 37 °C under 5% CO_2 for 24 h.

(1) Measurement of the Intracellular Nitrite Levels.

Briefly, cells were further incubated with lipopolysaccharides (LPS, 0.5 μg/mL), **PRO-ST** (20 μM)/LPS (0.5 μg/mL), Dex (20 μM)/LPS (0.5 μg/mL), TCOO (20 μM)/LPS (0.5 μg/mL). After the treatment, the cells were incubated for another 24 h. NO_2^- levels were measured by using a Griess Reagent Kit. The supernatant of the cell culture medium was collected and placed into a 96-well plate (100 μL per well), mixed with 100 μL of Griess reagent which was composed of equal volumes of N-(1-naphthyl)ethylenediamine (1 mg/mL) and sulfanilic acid (10 mg/mL) solution in 5% phosphoric acid). The plate was gently shaken for 15 min and the absorbance at 550 nm was recorded. Data were obtained from three independent experiments (n = 3). The nitrite levels were calculated according to the standard calibration curve.

(2) Measurement of Pro-inflammatory Cytokine Levels (TNF-α, IL-6)

The LPS (0.5 μg/mL)-pretreated cells were incubated with **PRO-ST** (20 μM), Dex (20 μM), and TCOO (20 μM) for 2 h. Thereafter, the cell culture supernatant (100 μL) was collected and the levels of TNF-α and IL-6 in each well were measured using a commercial ELISA kit according to the manufacturer's protocols.

1.7 NF-κB transactivation assay

NF-*κ*B DNA binding activity was further tested by a 96-well enzyme-linked immunosorbent assay (ELISA) from Abcam (ab176648). After the RAW 264.7 cells were treated with LPS (0.5 μg/mL) and **PRO-ST** (20 μM) for 24 h, 10 μL of cell nuclear extract (CelLytic™ Nu-CLEAR™ Extraction kit (Sigma)) was added to each well which has been coated with NF-*κ*B response element. NF-*κ*B DNA binding activity was measured using a commercial ELISA kit according to the manufacturer's protocols.

1.8 *In vivo* wound healing assay

The dorsal hair of BALB/c mice (6-8 weeks) was shaved. A full-thickness cutaneous wound (5 mm in diameter, Punch Biopsy; Miltex, York, Pennsylvania) was created on the dorsum of each mouse, one for the dynamic observation of wound healing and the other for histological testing. Then, 500 μL of **PRO-ST** gel (50 μM in sodium alginate, 5 ppm), TCOO gel (50 μM in sodium alginate, 5 ppm), PBS buffer, and chitin wound dressing were applied to the wounds every day, respectively. On days 0, 1, 3, 5, 7, 9, and 11, wounds were digitally photographed. One mouse per group was sacrificed on days 3 and 11, respectively. The wound and surrounding tissues (~ 5 mm) were collected for histological evaluation.

1.9 Histopathological study

10% Neutral buffered formalin was used to fix the wound and surrounding tissues. The fixed tissues were embedded in paraffin and sequentially sectioned at 5 μm using a Fitness ME microtome. Skin sections were stained with hematoxylin and eosin (H&E) for the evaluation of granulation tissue formation and wound maturity. All histological analyses were performed on at least 3 independent wounds per group, and the images displayed are representatives of all replicates. Images of entire sections were achieved on an IX71 microscope (Olympus).

1.10 Synthesis and Characterization of PRO-ST

2-(3-(4-hydroxystyryl)-5,5-dimethylcyclohex-2-en-1-ylidene)malononitrile (TCOO). To a solution of dicyanoisophorone (200 mg, 1.1 mmol) and 4-hydroxybenzaldehyde (131 mg, 1.1 mmol) in EtOH (5 mL) was added piperidine (0.04 mL). The reaction mixture was refluxed for 6 h. The solvent was removed under reduced pressure after cooling to room temperature. The crude product was purified by column chromatography on silica gel (petroleum ether/CH_2Cl_2, 1:4) to afford the compound **TCOO** as an orange solid (223.4 mg, 80% yield). ^{1}H NMR (400 MHz, DMSO-d_6): δ = 9.99 (s, 1H), 7.57 (d, J = 8.8 Hz, 2H), 7.21 (d, J = 4.4 Hz, 2H), 6.81 - 6.79 (d, J = 8.8 Hz, 2H), 6.80 (s, 1H), 2.60 (s, 2H), 2.53 (s, 2H), 1.01 (s, 6H); ^{13}C NMR (100 MHz, $CDCl_3$): δ = 169.51, 157.37, 154.48, 136.92, 129.40(2C), 128.51,

126.95, 122.69, 116.09(2C), 113.68, 112.93, 77.59, 43.00, 39.19, 32.02, 28.00(2C). HRMS (ESI): calcd for $C_{19}H_{18}N_2O$ $[M-H]^-$ *m/z* 289.1335, found 289.1254.

O-(4-(2-(3-(dicyanomethylene)-5,5-dimethylcyclohex-1-en-1-yl)vinyl)phenyl) carbonochloridothioate (3). The compound **TCOO** (250 mg, 0.75 mmol) was dissolved in THF (5 mL). KOH (56 mg, 1 mmol) dissolved in 0.5 mL deionized water was added to the above solution. Then the solution was stirred at room temperature for 10 min. The above solution was dropwise added into a solution of tiophosgene (760, 8 mmol) in anhydrous THF, then the reaction mixture was stirred for 1h at room temperature under nitrogen. The solution and remaining thiophosgene were removed under nitrogen. The crude product was purified by column chromatography on silica gel (petroleum ether/CH_2Cl_2, 1:1) to obtain compound **3** as an orange solid (209.5 mg, 57%). ^{1}H NMR (400 MHz, $CDCl_3$): δ = 7.57 (d, *J* = 8.4 Hz, 2H), 7.18 (d, *J* =8.8 Hz, 2H), 7.02 (q, *J* = 16.4 Hz, 2H), 6.85 (s, 1H), 2.60 (s, 2H), 2.46 (s, 2H), 1.08 (s, 6H); ^{13}C NMR (100 MHz, $CDCl_3$): δ = 185.41, 169.04, 154.96, 153.10, 134.99, 134.91, 130.25, 128.86(2C), 124.13, 121.87(2C), 113.24, 112.48, 79.33, 42.87, 39.09, 31.96, 27.92(2C). HRMS (ESI): calcd for $C_{20}H_{17}ClN_2OS$ $[M-H]^-$ *m/z* 367.0666, found 367.0844.

(4-isothiocyanatophenyl)methanol (2). Tiophosgene (150 μL, 2 mmol) was slowly added to a solution of compound **1** (123 mg, 1 mmol) in anhydrous CH_2Cl_2 (2 mL). The reaction mixture was stirred for 0.5 h at room temperature under nitrogen. After the solvent was evaporated, the crude product was further purified by the silica gel column chromatography (petroleum ether/EtOAc, 5:1) to yield compound **2** as a white solid (114.6 mg, 69%). ^{1}H NMR (400 MHz, $CDCl_3$): δ = 7.34 (d, *J* = 8.8 Hz, 2H), 7.23 (d, *J* = 8.4 Hz, 2H), 4.69 (s, 2H), 1.74 (s, 1H); ^{13}C NMR (100 MHz, $CDCl_3$): δ = 140.08, 135.23, 130.32, 127.89(2C), 125.78(2C), 64.39. HRMS (ESI): calcd for $C_8H_7NOS[M-H]^-$ *m/z* 164.0165, found 164.0346.

PRO-ST. Compound **2** (36 mg, 0.22 mmol) and DMAP (53 mg, 0.44 mmol) were dissolved in anhydrous CH_2Cl_2 (5 mL). Compound **3** (80 mg, 0.22 mmol) dissolved in 1 mL anhydrous CH_2Cl_2 was added to the above solution. The mixture was stirred for 10 min at room temperature. After completion of the reaction, the resulting

solution was purified immediately through silica column chromatography (petroleum ether /CH_2Cl_2, 1:1) to give the desired **PRO-ST**. ^{1}H NMR (400 MHz, $CDCl_3$): δ = 7.55 (d, J = 8.8 Hz, 2H), 7.44 (d, J = 8.4 Hz, 2H), 7.28 (d, J = 8.4 Hz, 2H), 7.16 (d, J = 8.8 Hz, 2H), 7.02 (q, J = 16.0 Hz, 2H), 6.85(s, 1H), 5.54 (s, 2H), 2.61 (s, 2H), 2.46 (s, 2H), 1.08 (s, 6H); ^{13}C NMR (100 MHz, $CDCl_3$): δ = 194.31, 169.12, 153.99, 153.31, 136.34, 135.45, 134.25, 133.19, 131.75, 129.82, 129.73(2C), 128.67(2C), 126.01(2C), 123.97, 122.67(2C), 113.34, 112.59, 79.19, 74.56, 42.96, 39.18, 32.02, 27.99(2C). HRMS (ESI): calcd for $C_{28}H_{23}N_3O_2S_2$ $[M\text{-}H]^-$ *m/z* 496.1148, found 496.1155.

Table S1. Summary of activatable H_2S donors.

Fluorescent H_2S donors	Activation type	Optical parameters	H_2S detecting method	H_2S releasing efficiency	Ref
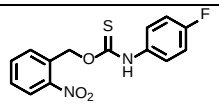	UV Light (365 nm)	-	Methylene blue assay	[a]N.F.	*Org. Lett.* **2017**, *19*, 2278−2281
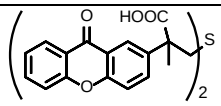	UV Light (325–385 nm)	-	Methylene blue and HSip-1 assay	N.F.	*Bioorg. Med. Chem. Lett.* **2015**, *25*, 175−178
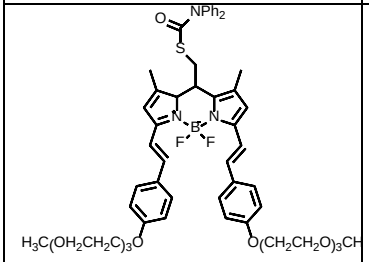	VIS-NIR (700 nm)	$\lambda_{ex/em}$= 688/779 nm	Methylene blue and SF7-AM assay	48%	*Org. Lett.* **2018**, *20*, 4907−4911
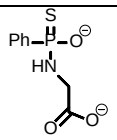	pH	-	Methylene blue assay	N.F.	*J. Am. Chem. Soc.* **2016,** *138*, 6336−6339
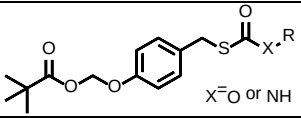	Esterase	-	Dn-N3-based assay	N.F.	*Org. Lett.* **2017**, *19*, 62−65
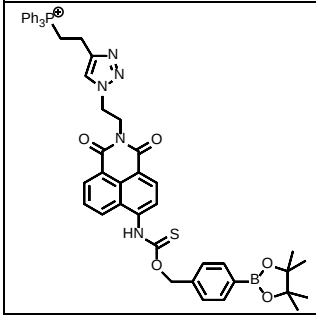	ROS	$\lambda_{ex/em}$= 405/540 nm	Methylene blue assay	N.F.	*ACS Sens.* **2020,** *5*, 319−326

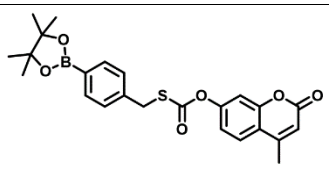	ROS	$\lambda_{ex/em}$= 365/448 nm	Methylene blue assay	N.F.	*Tetrahedron Lett.* **2021,** *69*, 152944
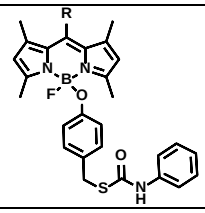	Visible-Light (λ=470 nm)	$\lambda_{ex/em}$= 470/540 nm	Methylene blue and H_2S-sensitive electrode assay	30%~40%	*Org. Lett.* **2017**, *19*, 4822−4825
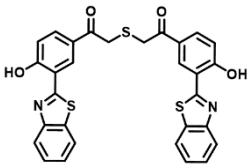	UV-Vis light (λ>410 nm)	From green ($\lambda_{ex/em}$=350/ 517 nm)to blue ($\lambda_{ex/em}$= 350/450 nm)	Coumarin-hemicyanine fluorescence dye and methylene blue assay	N.F.	*Chem. Commun.* **2018**, *54*, 3106
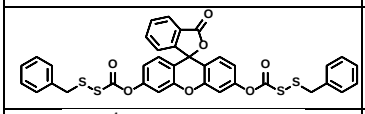	Cys	$\lambda_{ex/em}$= 490/520 nm	Methylene blue assay	75%	*Chem. Sci.* **2019**, *10*,1873−1878
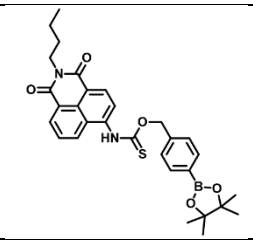	ROS	$\lambda_{ex/em}$= 405/577 nm	Methylene blue assay	N.F.	*Chem. Sci.* **2019,** *10*, 7690−7694
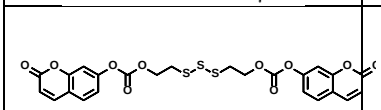	Biothiol	$\lambda_{ex/em}$= 332/446 nm	Fluorescent probe NAP-1 and methylene blue assay	N.F.	*Chem. Commun.* **2020**, *56*, 7769−7772
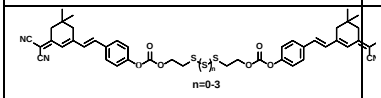	Thioredoxin reductase	$\lambda_{ex/em}$= 580/670 nm	Fluorescent probe WSP-2 and methylene blue assay	N.F.	*J. Mater. Chem. B* **2022**, *10*, 2183−2193
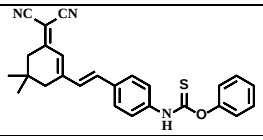	Cys	$\lambda_{ex/em}$= 470/660 nm	H_2S fluorescent probe C-7AZ	62%	*Anal. Chem.* **2021**, *93*, 4894−4901
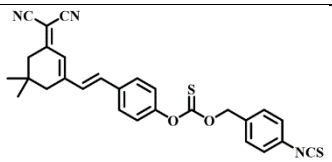	Biothiols	$\lambda_{ex/em}$= 530/666 nm	H_2S fluorescent probe C-7AZ and methylene blue assay	72.9%	**This work**

[a]N.F. means “Not Find”.

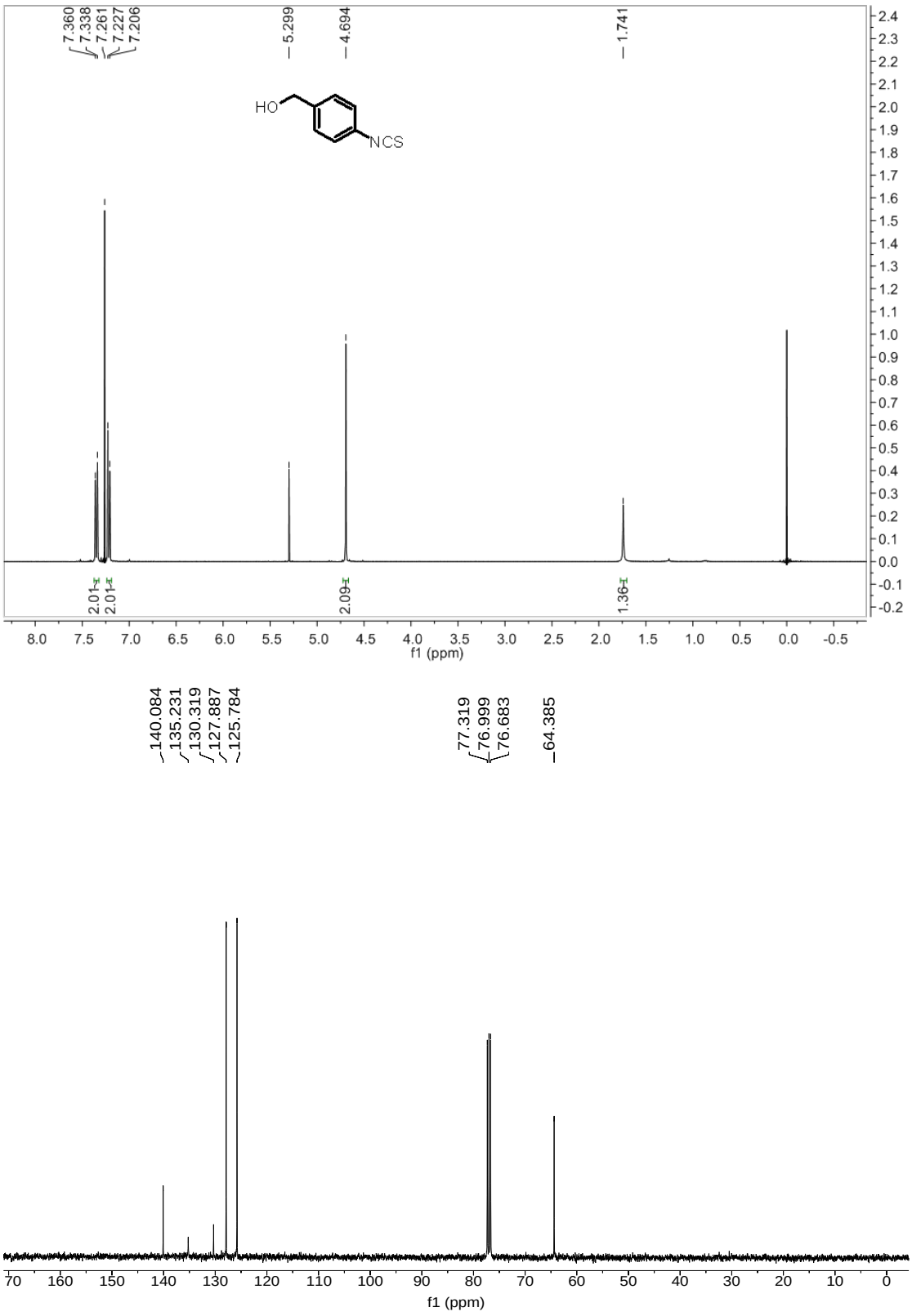

Figure S1. ^{1}H-NMR and ^{13}C-NMR spectrum of **2** in $CDCl_3$ (400 MHz).

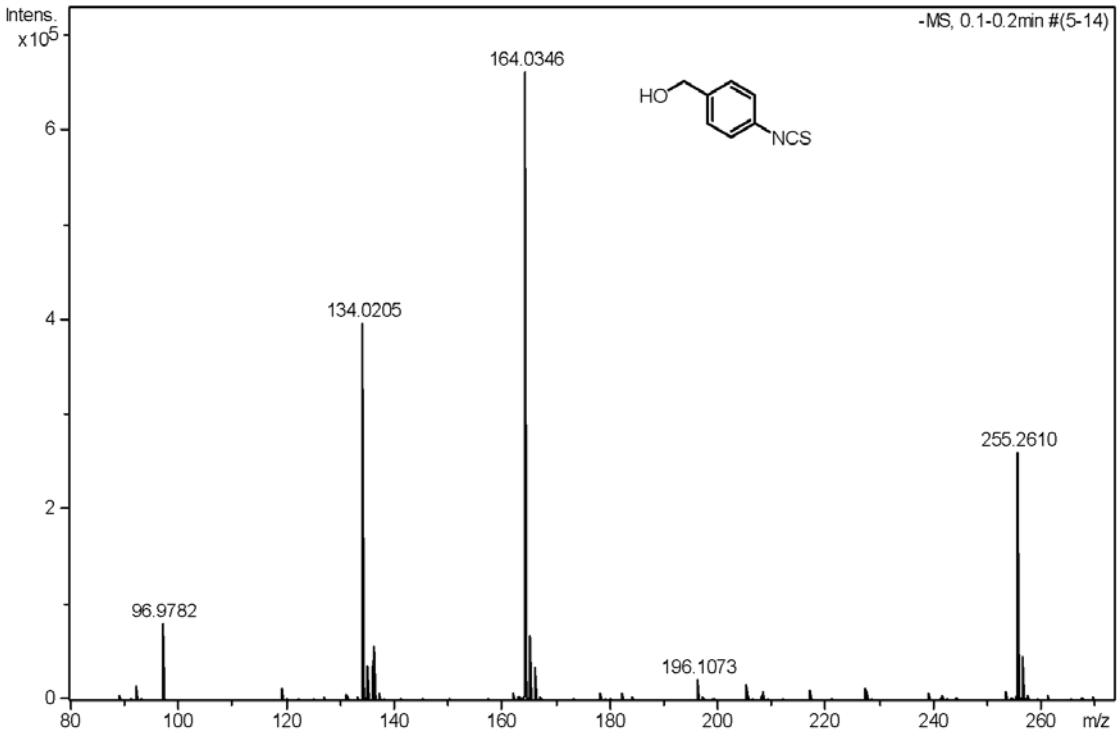

Figure S2. HRMS (ESI) spectrum of **2**.

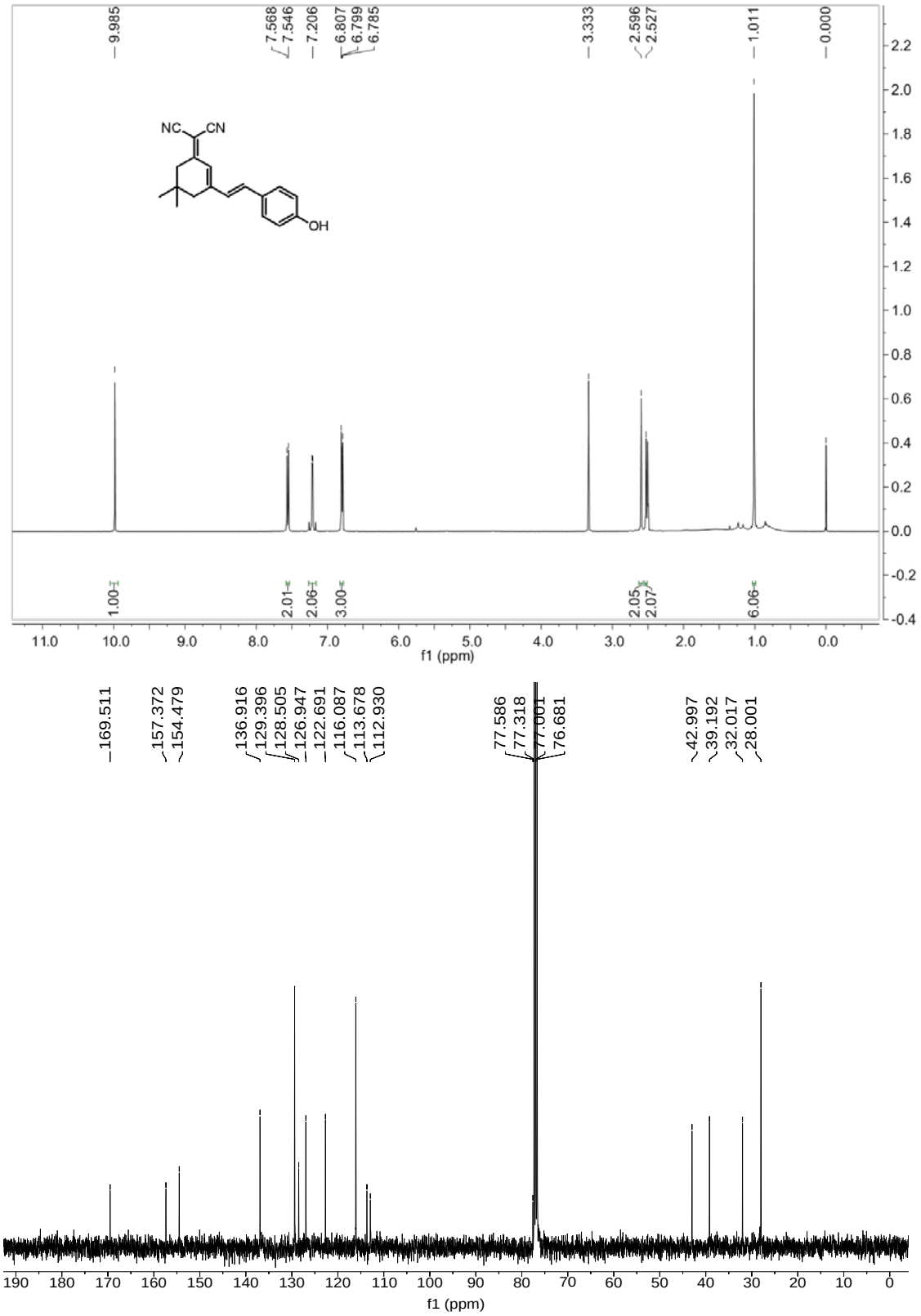

Figure S3. ^{1}H-NMR spectrum of **TCOO** in DMSO-d_6 (400 MHz).

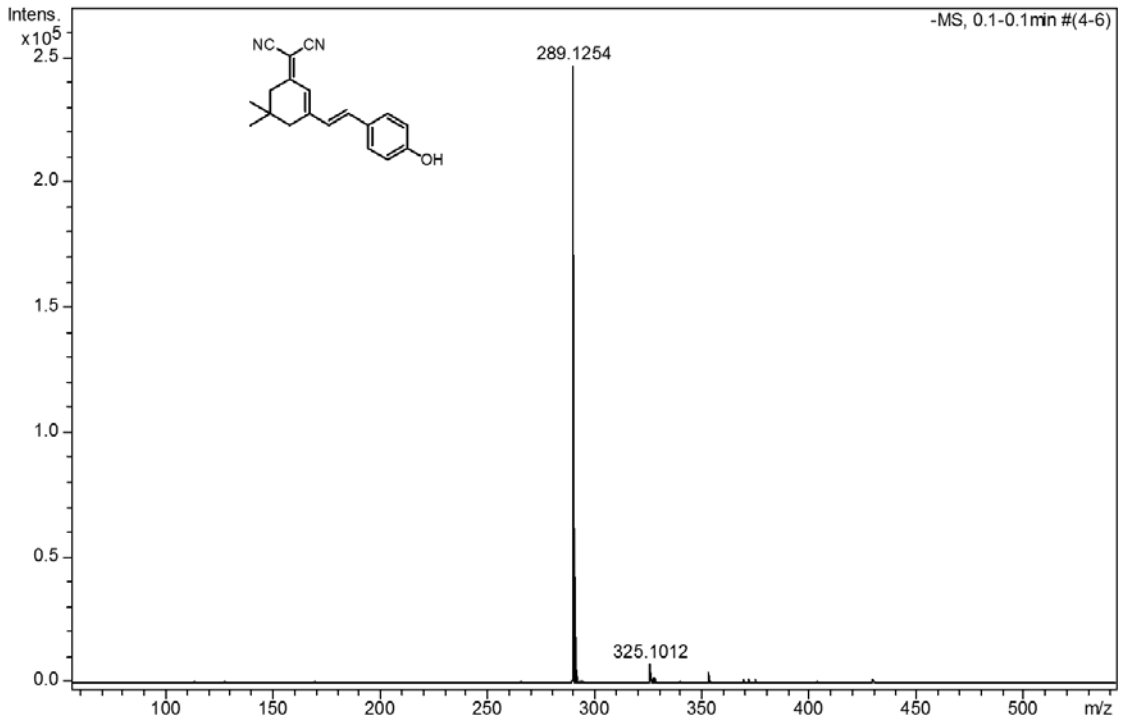

Figure S4. HRMS (ESI) spectrum of **TCOO**.

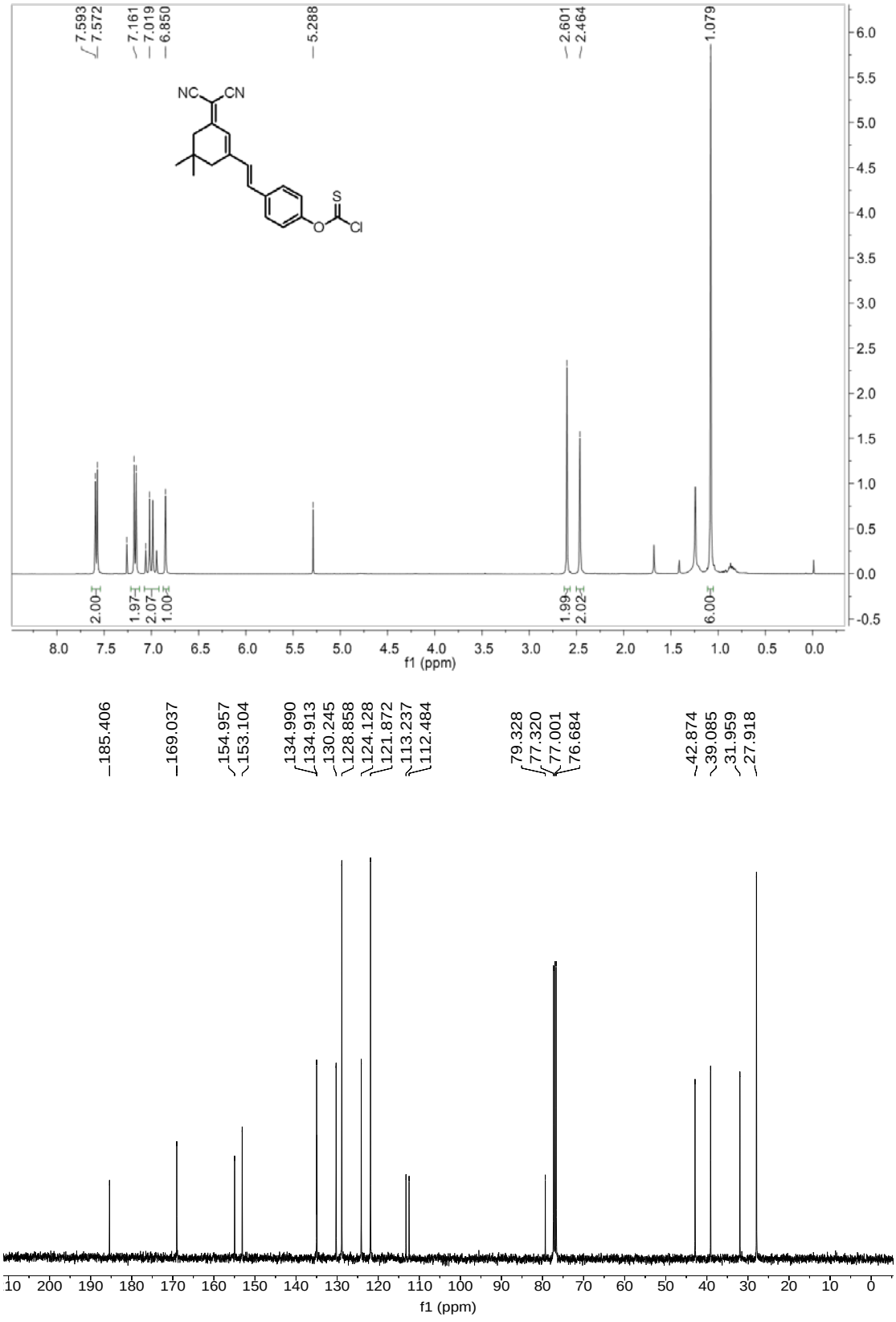

Figure S5. ^{1}H-NMR spectrum of **3** in $CDCl_3$ (400 MHz).

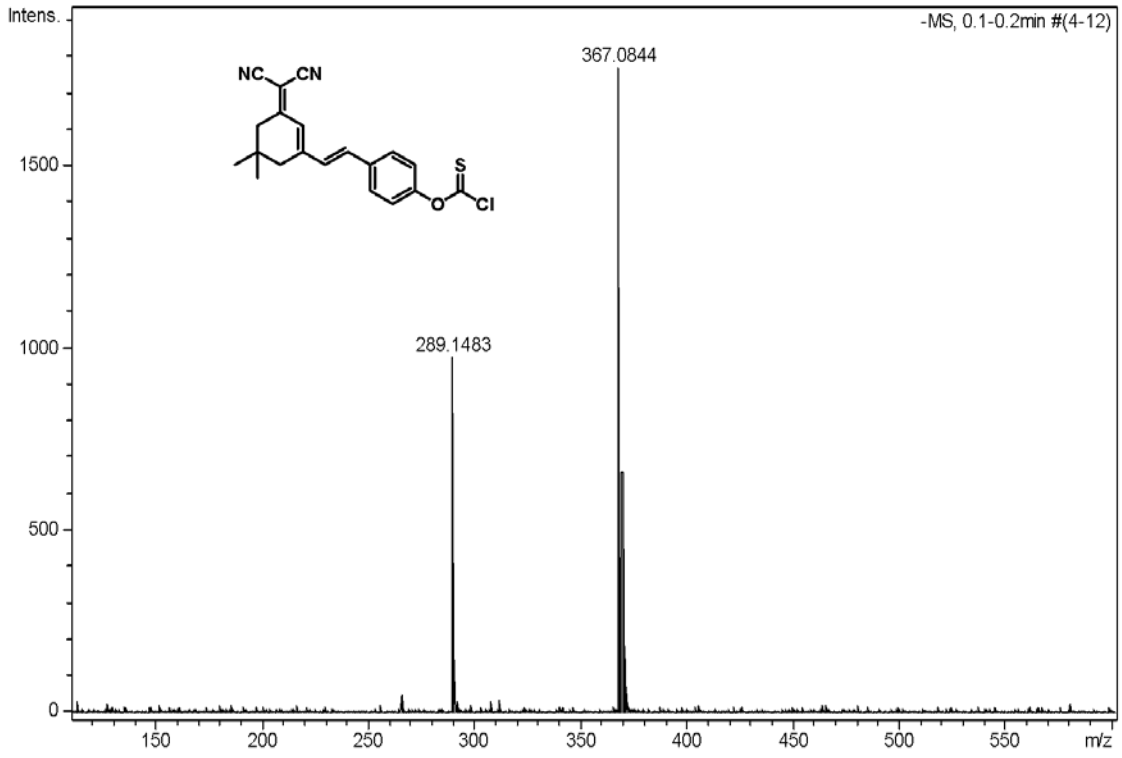

Figure S6. HRMS (ESI) spectrum of **3**.

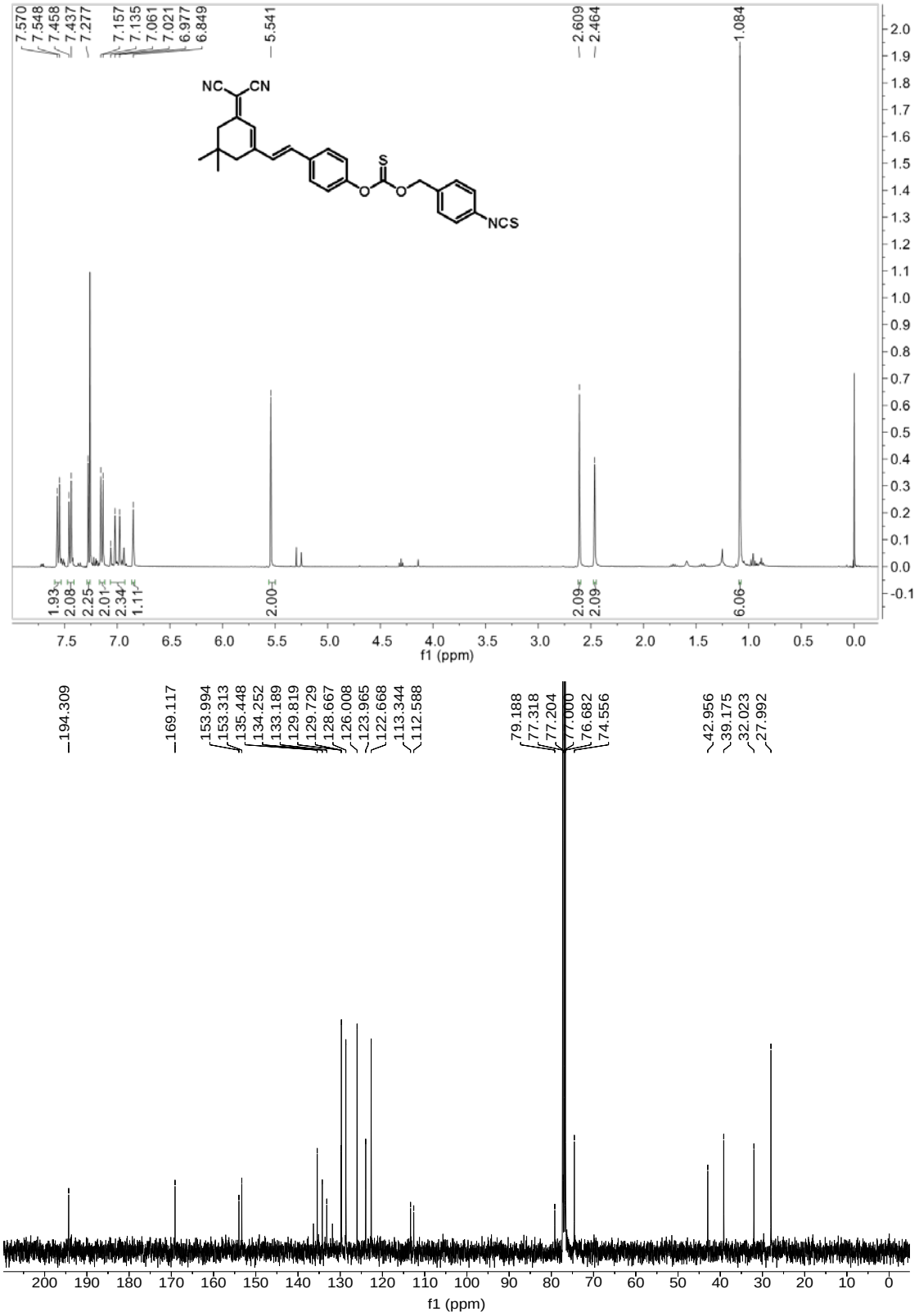

Figure S7. ^{1}H-NMR spectrum of **PRO-ST** in $CDCl_3$ (100 MHz).

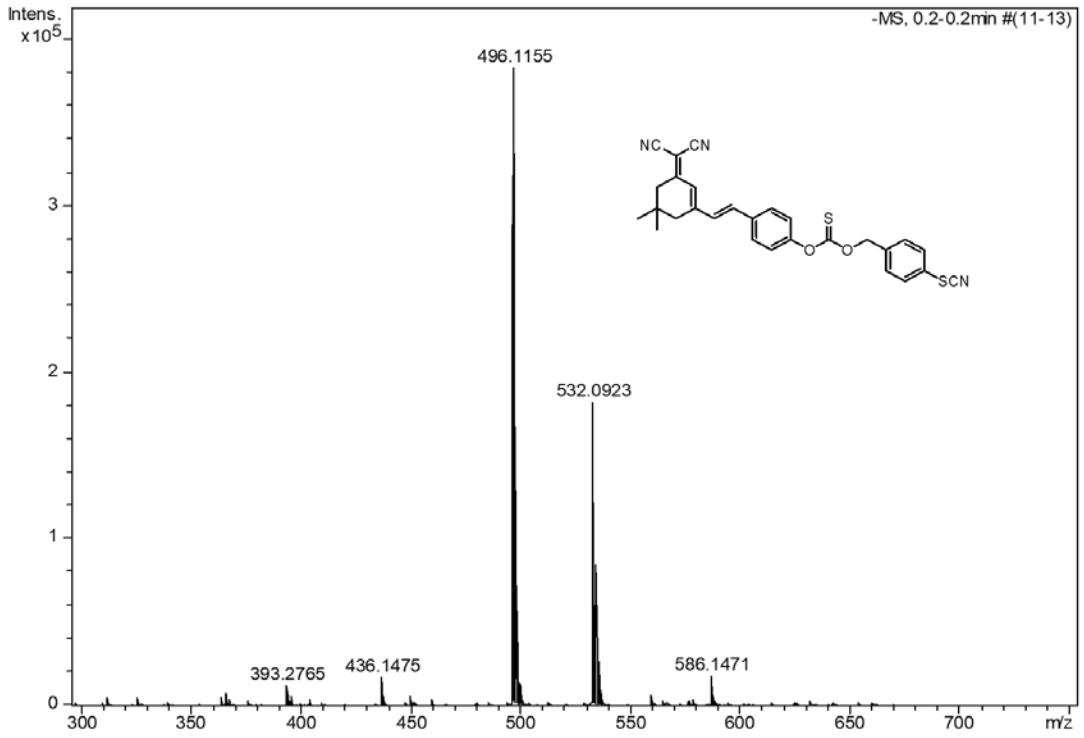

Figure S8. HRMS (ESI) spectrum of **PRO-ST**.

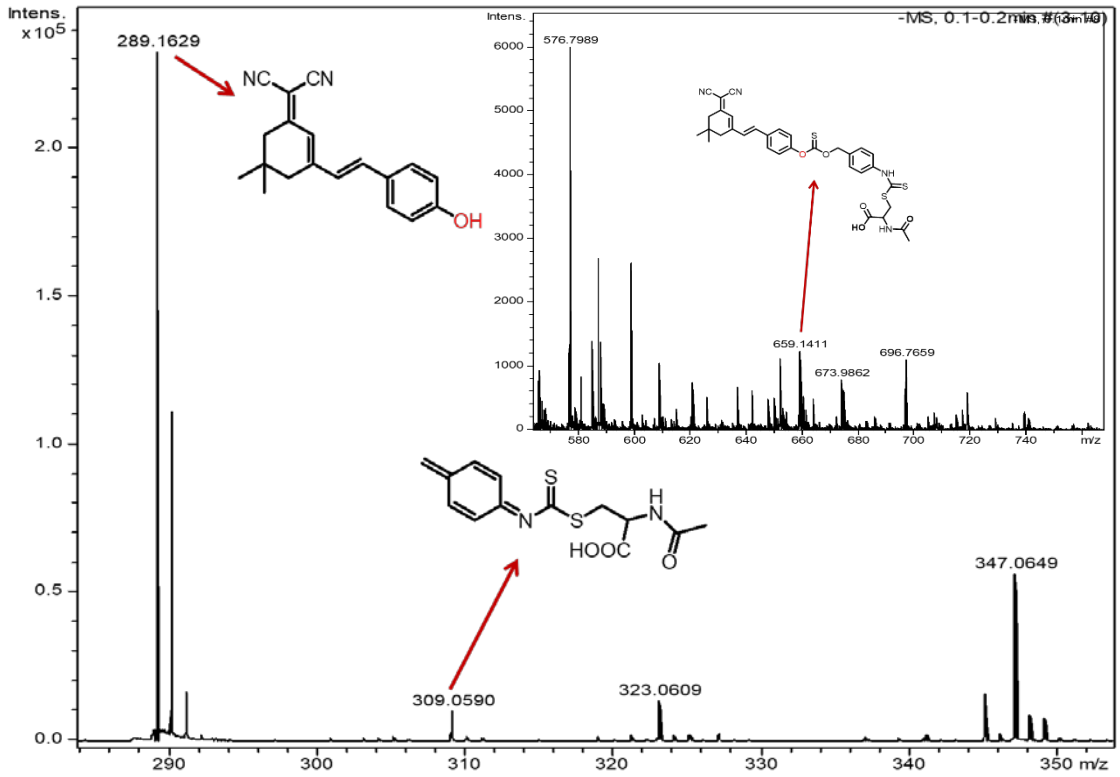

Figure S9. Mass spectrometry schematic diagram of **PRO-ST** response mechanism to NAC.

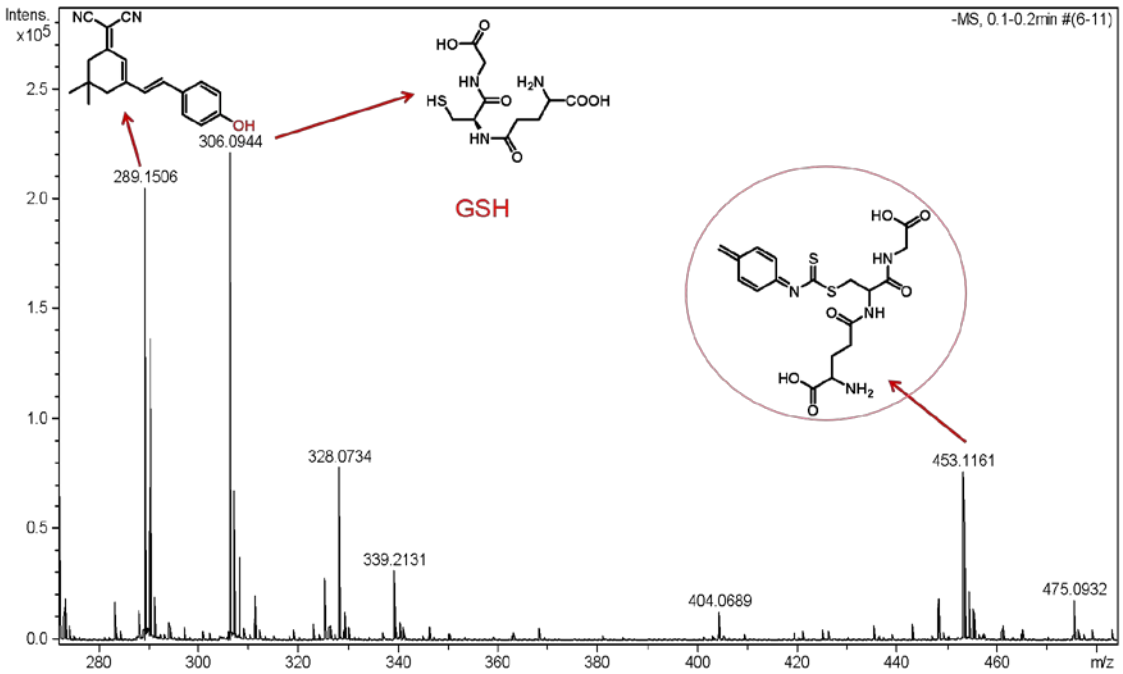

Figure S10. Mass spectrometry schematic diagram of **PRO-ST** response mechanism to GSH.

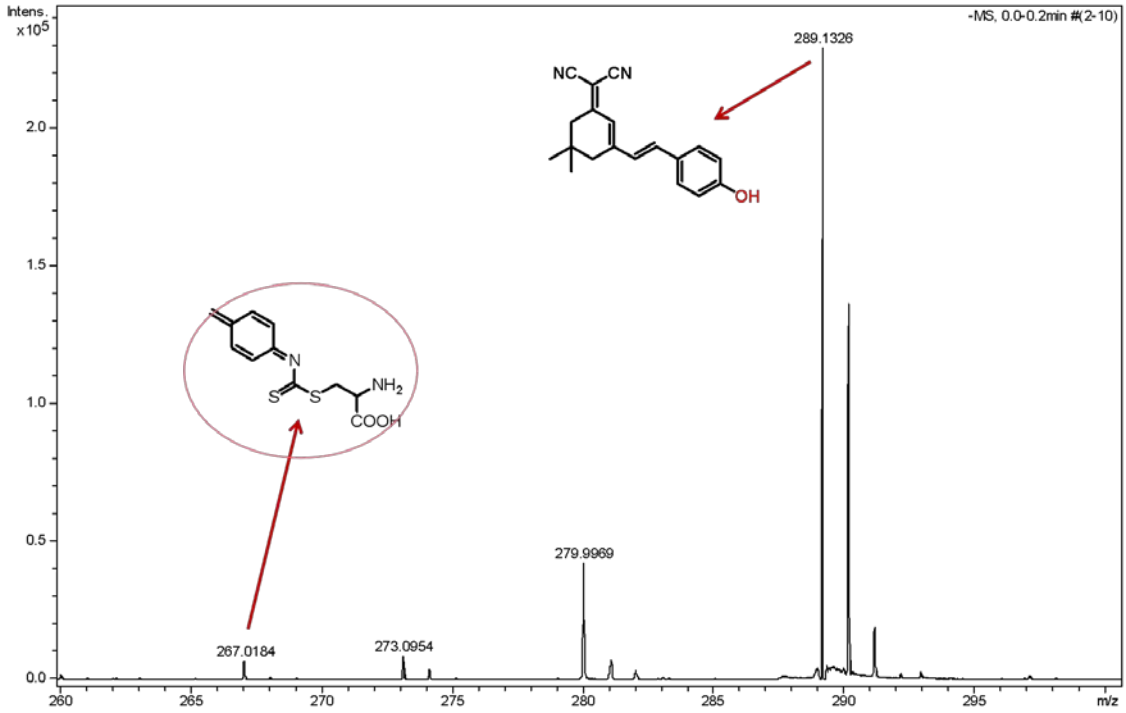

Figure S11. Mass spectrometry schematic diagram of **PRO-ST** response mechanism to Cys.

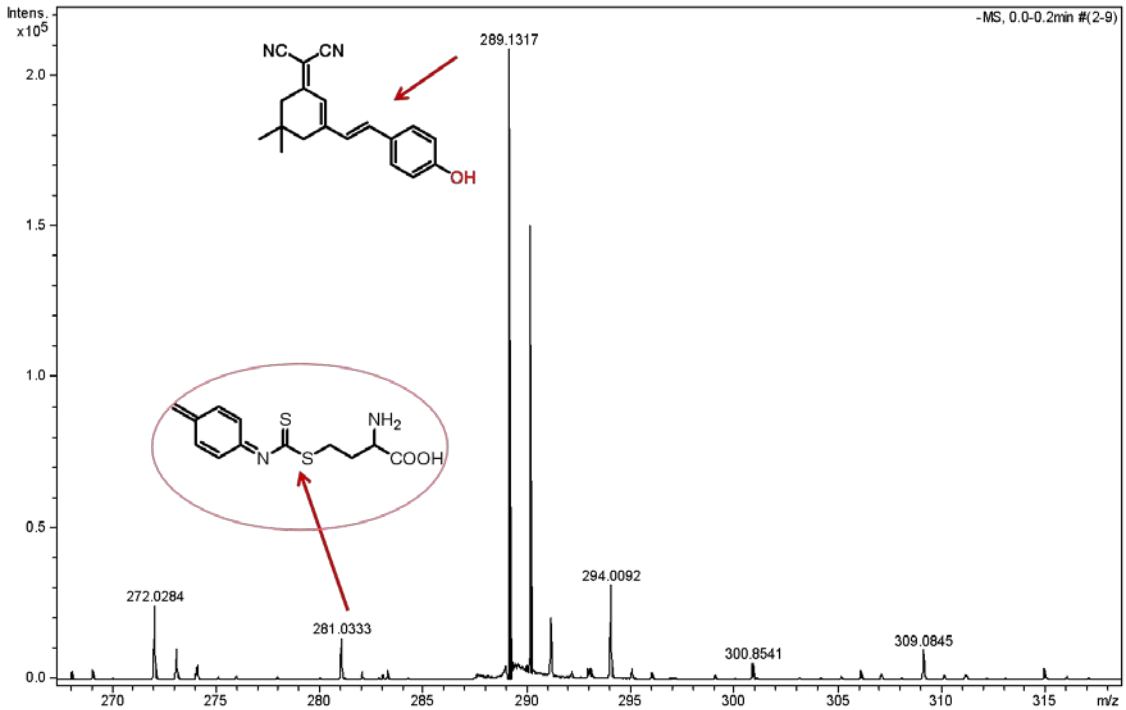

Figure S12. Mass spectrometry schematic diagram of **PRO-ST** response mechanism to Hcy.

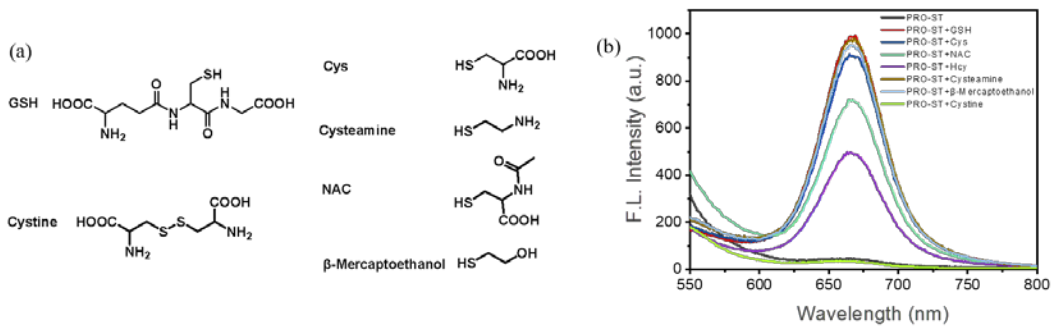

Figure S13. (a) The structure of thiol compounds. (b) Fluorescence spectra of **PRO-ST** (10 μM) in the presence of GSH, Cys, Hcy, NAC, *β*-Mercaptoethanol, Cysteamine, and Cystine (200 μM), respectively. Conditions: DMF/PBS (pH = 7.4, 20 mM, *v/v*, 3/7) at 37 ^{o}C for 30 min. Slit (nm): 5/10, λ_{ex} = 530 nm.

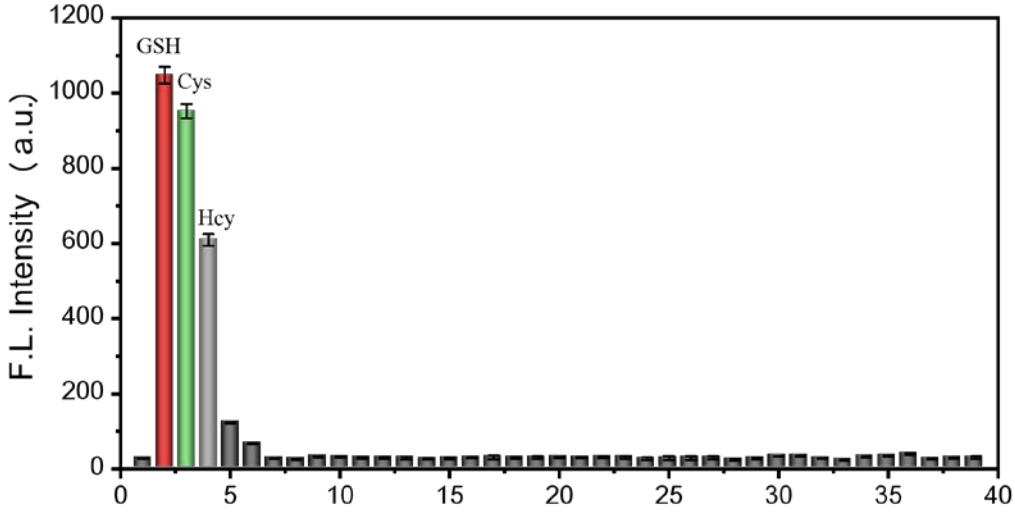

Figure S14. Fluorescence intensity of **PRO-ST** (10 μM) at 666 nm toward different species (200 μM) including biothiols (GSH/Cys/Hcy), H_2S, BSA, 16 amino acids (Arg, Ser, Gly, Val, Tyr, Leu, His, Pro, Glu, Thr, Asp, Phe, Asn, Lys, Met, Ile), 10 cations (K^+, Na^+, Ca^{2+}, Mg^{2+}, Cu^{2+}, Zn^{2+}, Hg^{2+}, Al^{3+}, Fe^{3+}, and Fe^{2+}), 7 reactive oxygen/nitrogen species (RONS) ($^1O_2$, $O_2^{\cdot-}$, H_2O_2, ClO^-, ·OH, $ONOO^-$, NO_2^-).

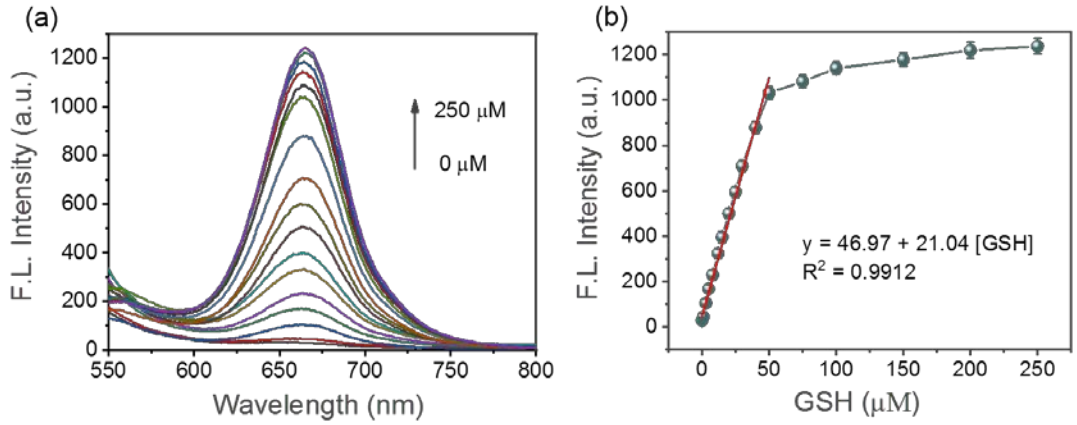

Figure S15. (a) Fluorescence spectra of **PRO-ST** (10 μM) in the presence of increasing concentrations of GSH (0 − 250 μM). (b) The linear changes of the fluorescence intensity of **PRO-ST** at 666 nm and as a function of GSH concentration. Conditions: DMF/PBS (pH = 7.4, 20 mM, *v/v*, 3/7) at 37 °C for 30 min. Slit (nm): 5/10. λ_{ex} = 530 nm.

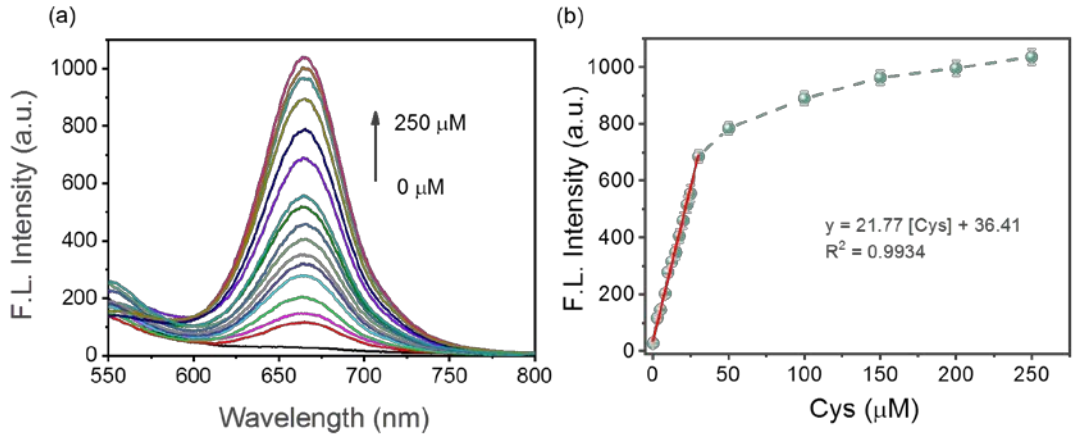

Figure S16. (a) Fluorescence spectra of **PRO-ST** (10 μM) in the presence of increasing concentrations of Cys (0 − 250 μM). (b) The linear changes of the fluorescence intensity of **PRO-ST** at 666 nm and as a function of Cys concentration.

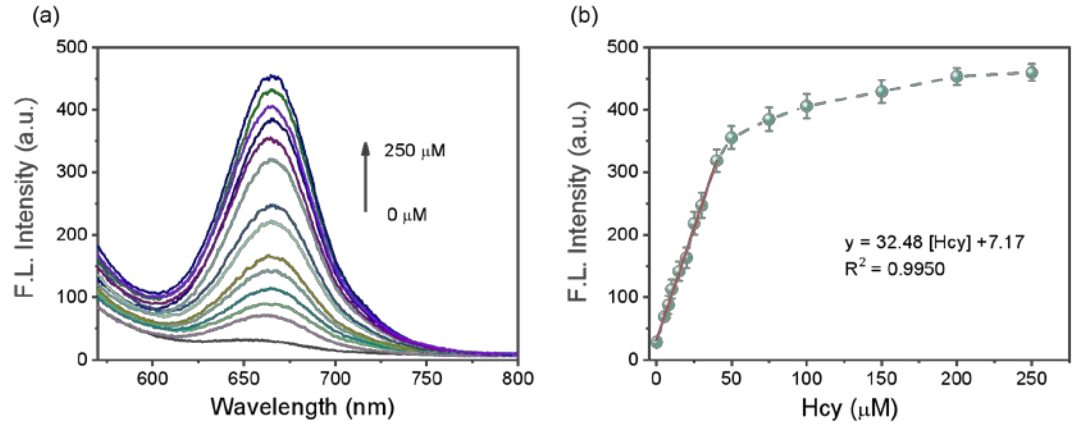

Figure S17. (a) Fluorescence spectra of **PRO-ST** (10 μM) in the presence of increasing concentrations of Hcy (0 − 250 μM). (b) The linear changes of the fluorescence intensity of **PRO-ST** at 666 nm and as a function of Hcy concentration.

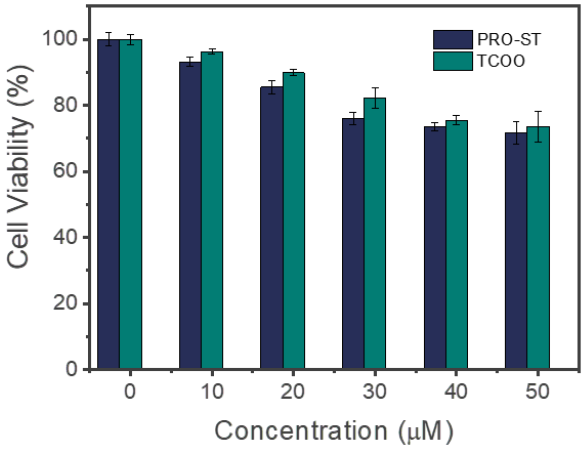

Figure S18. Cell cytotoxicity of **PRO-ST**, TCOO against RAW 246.7 cells evaluated by MTT assay. The results are expressed as mean ± SD (n = 6).

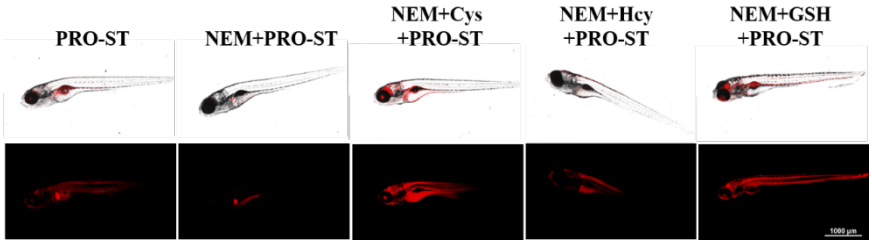

Figure S19. Confocal fluorescence images of zebrafish. (First column) the zebrafishes were incubated with **PRO-ST** (10 μM) for 30 min; (Second column) the NEM-zebrafish pretreated with **PRO-ST** (10 μM) for 30 min ; (Third-Fifth column) NEM-pretreated zebrafishes were incubated with Cys (100 μM), Hcy (100 μM), and GSH (100 μM) for 30 min, respectively, and then with **PRO-ST** (10 μM) for 30 min. Red channel: λ_{ex} = 514 nm, λ_{em} = 620 - 700 nm.

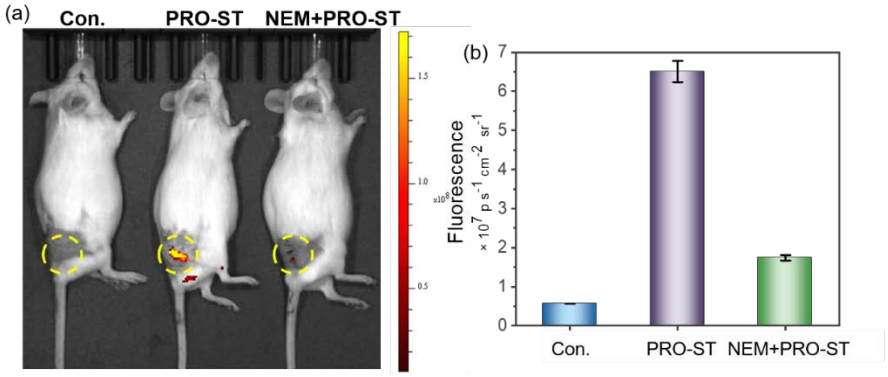

Figure S20. (a) Fluorescent imaging of thiols in live mice with saline (25 μL)/ **PRO-ST** (10 mM, 25 μL)/NEM (100 mM, 25 μL) and **PRO-ST** (10 mM, 25 μL); (b) Fluorescent intensity from the circle area of mice in (a). λ_{ex} = 530 nm, λ_{em} = 660 nm.

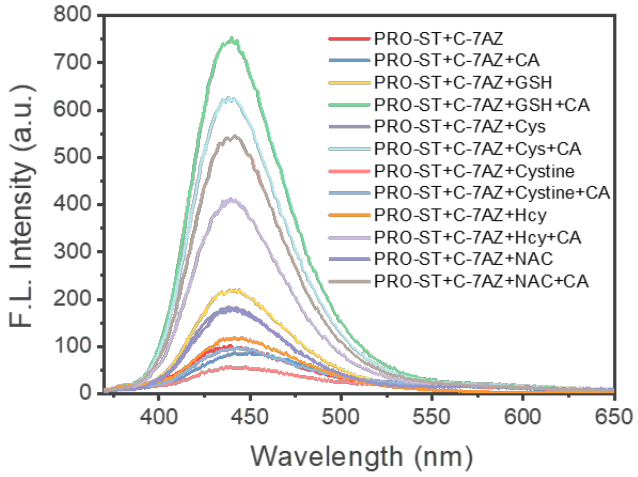

Figure S21. Fluorescence emission spectra of **C-7AZ** (3 μM) upon addition of **PRO-ST** (10 μM), thiols (100 μM), and carbonic anhydrase (CA, 25 μg/mL). (λ_{ex} = 350 nm)

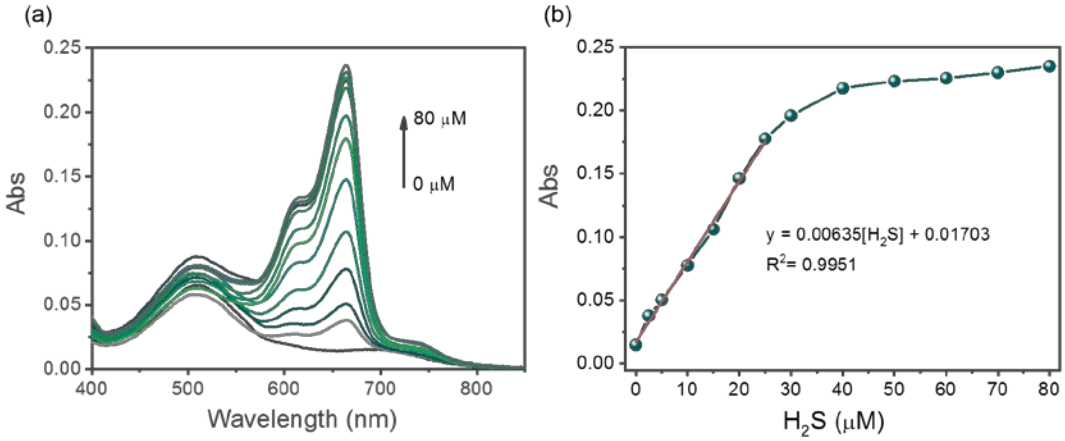

Figure S22. (a) Absorption spectra of MB in the presence of increasing concentrations of H_2S (0 - 80 μM). (b) The linear changes of the absorption intensity of MB at 667 nm and as a function of H_2S concentration.

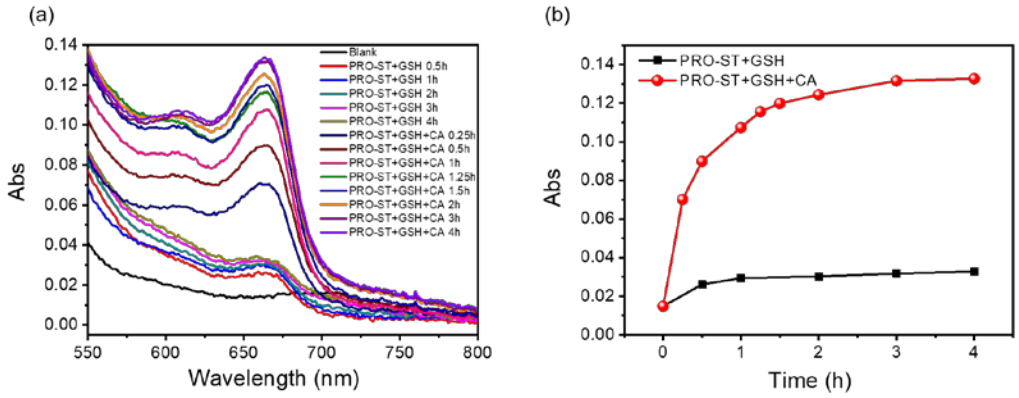

Figure S23. (a) Time-dependent absorption spectra of MB in the presence of **PRO-ST** (25 μM), GSH (250 μM), and CA (25 μg/mL). (b) Time-dependent absorption intensity of MB (200 μM) reacted with **PRO-ST**, GSH, and CA at 667 nm.

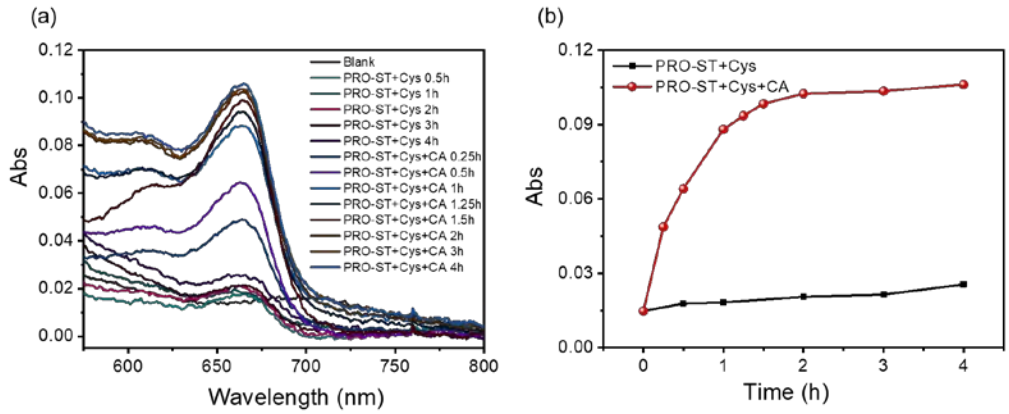

Figure S24. (a) Time-dependent absorption spectra of MB in the presence of **PRO-ST** (25 μM), Cys (250 μM), and CA (25 μg/mL). (b) Time-dependent absorption intensity of MB reacted with **PRO-ST**, Cys, and CA at 667 nm.

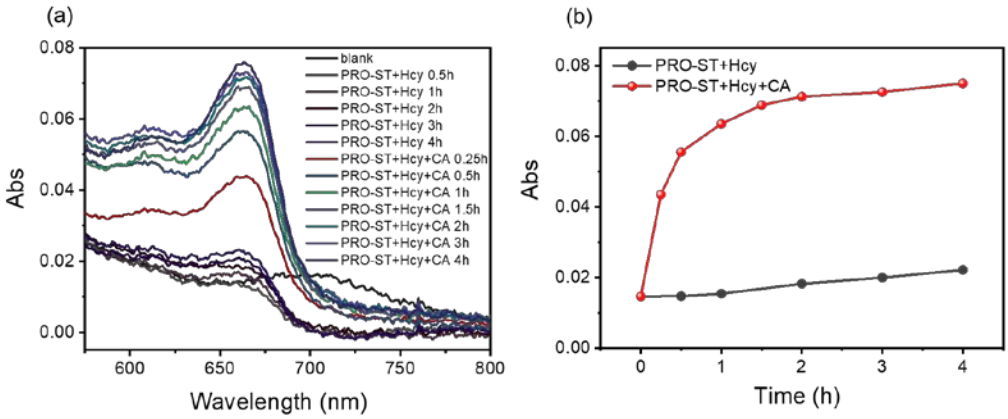

Figure S25. (a) Time-dependent absorption spectra of MB in the presence of **PRO-ST** (25 μM), Hcy (250 μM), and CA (25 μg/mL). (b) Time-dependent absorption intensity of MB reacted with **PRO-ST**, Hcy, and CA at 667 nm.